Usefulness of clearance parametric images in detection of regional renal parenchyma dysfunction

Jacek Kuśmierek[1], Małgorzata Bieńkiewicz[2], Tomasz Konecki[3], Marian Surma[1], Marek Sosnowski[3], Anna Płachcińska[2]

[1]Department of Nuclear Medicine, Medical University of Łódź, Poland
[2]Department of Quality Control and Radiological Protection, Medical University of Łódź, Poland
[3]1ˢᵗ Department of Urology, Medical University of Łódź, Poland

Abstract

BACKGROUND: The aim of the study was to examine whether parametric clearance images (PAR) enhance diagnostic potential of a dynamic renal scintigraphy with detection of local dysfunction of kidneys, on a model of kidneys after treatment with extracorporeal shock wave lithotripsy (ESWL),

MATERIAL AND METHODS: Kidneys after ESWL were accepted as a proper model for the implementation of this objective because of the previously proven damaging effect of a shock wave on renal parenchyma and known region of ESWL application. Forty patients (23 males and 17 females) at the age of 37 to 70 years (mean value 54) with untreated earlier single, one-sided nephrolithiasis, currently treated with ESWL, underwent a study. A dynamic renal ^{99m}Tc-EC scintigraphy was performed three times: before ESWL, a week and a month after this therapeutic intervention. PAR images generated with use of an in-house developed software were compared with summation (SUM) of images obtained from radiopharmaceutical uptake phase and quantitative global function parameters (GFP) of each kidney, like split function, MTT — mean transit time and PTT — parenchymal transit time.

RESULTS: PAR and SUM images of all 40 kidneys before ESWL were normal. PAR images revealed local or diffused defects a week and a month after therapeutic intervention in statistically significantly larger numbers of kidneys than SUM images (19 vs. 6, p = 0.002 and 16 vs. 5, p = 0.003, respectively). A week after ESWL, when defects in PAR images were observed in about a half of all renal segments (29/57 — 51%) all GFP values were significantly worse than in kidneys without defects. A month after ESWL defects in PAR images could be observed in ab. 1/3 (17/48 — 35%) of segments and were less extensive, whereas GFP values did not differ significantly from values in kidneys without clearance function impairment in the PAR images.

CONCLUSIONS: PAR images enhance diagnostic potential of a dynamic renal scintigraphy with detection of local function defects. These images allow to detect more local renal function defects than SUM images.

KEY words: dynamic renal scintigraphy, parametric renal clearance images, extracorporeal shock wave lithotripsy

Nucl Med Rev 2017; 20, 1: 39–44

Background

Dynamic renal scintigraphy provides qualitative and quantitative data on a global radiopharmaceutical uptake function of each kidney and transport function through urinary tract. It does not, however, allow to evaluate a regional parenchyma dysfunction with accuracy close to that of a static renal scintigraphy, especially acquired with a SPECT study.

Parametric images obtained from radionuclide studies provide images of regional distribution of parameters specific for organ function. First parametric images of renal clearance function were generated by Oppenheim et al. [1] and Szabo et al. [2]. The method used in our department for generation of such images based on Rutland-Patlak analysis method [3] was presented earlier [4].

The objective of the work was to find out whether clearance parametric images enhance diagnostic power of a dynamic renal scintigraphy with detection of local kidney dysfunction. We accepted kidneys after extracorporeal shock wave lithotripsy (ESWL) as a proper model for implementation of this objective because of proven earlier damaging effect of a shock wave on renal parenchyma and known region of ESWL application. After many years of therapeutic application of ESWL its traumatic side effect on renal parenchyma is apparent. Histological examinations revealed damages to nephrons and also small and medium arteries around

Correspondence to: Anna Płachcińska
Department of Quality Control and Radiological Protection,
Central Teaching Hospital
Czechosłowacka 8/10 street, 92–216 Łódź, Poland
Tel: +48 42 6783684; Fax: +48 42 6757285
E-mail: anna.plachcinska@umed.lodz.pl

a focus of ultrasound wave [5, 6]. Diagnostic imaging performed shortly after ESWL revealed hematoma or acute intrarenal edema [7, 8]. It is believed that an oxidative stress resulting from tissue hypoperfusion is followed by a local inflammatory reaction — lithotripsy nephritis [9]. Transient functional damage after ESWL may also involve a whole kidney [10, 11].

Material and methods

Subjects

In order to provide a material homogeneity in accordance with an accepted model, a study material was selected from among patients referred to our department with indication to assess renal damage and patency of urinary tract, before and after ESWL treatment. An ESWL intervention was performed using a Siemens Lithostar Modularis Vario device, with application of a 60–120 s⁻¹ frequency shock wave and 2000–4500 impulses emitting a total energy of 50J. The study was approved by the Medical University Bioethics Committee and all the subjects signed a written informed consent. Patients with a single, one-sided nephrolithiasis that was not treated earlier, with renal calculus in the range between 8 and 20 mm (in accordance with recommendations of European Association of Urology) were qualified for the study material. Previous surgical treatment of urinary system, nephrolithiasis causing urinary tract blockage, renal malformations, urinary infections, ureter catheters, nephrostomy and other diseases affecting renal function, like diabetes, systemic diseases and hypertension, were considered as factors excluding from this study. Patients with urinary tract blockage revealed after ESWL in ultrasonographic study before a radionuclide control examination were also excluded from the studied material. In effect, 40 patients (23 males and 17 females) at the age of 37 to 70 (mean value 54) years underwent a study.

Altogether 40 kidneys after ESWL were evaluated. In 25 of them a calculus was located in a calix (in 12 in upper, 3 — medium and 10 — lower) and in 15 kidneys — in pelvis.

Data acquisition

A dynamic renal scintigraphy was performed three times: before ESWL, a week and a month after this therapeutic intervention, with a Nucline AP camera (Mediso Medical Imaging Systems) equipped with a low energy general purpose collimator. Dynamic acquisition in posterior projection was performed after intravenous injection of 111 MBq of ^{99m}Tc-etylenedicysteine (EC). Patients drank 10 ml of water per kilogram of body mass to attain a proper hydration before radiopharmaceutical injection. As a result a sequence of sixty 20-second images in a 64 x 64 matrix with zoom equal to 1.5 were obtained.

Data analysis

Time-activity curves were generated from both kidneys, heart and extra-renal background between both kidneys.

A conventional evaluation a global function of each kidney was performed using a summed image (SUM) of 40 to 140 seconds of a study, after a standard background correction, complemented with quantitative parameters reflecting this function: a split function (SF) and transit times obtained after deconvolution of renal curves: mean (MTT), through a whole kidney and parenchymal

(PTT) [12, 13]. Deconvolution of curves was performed using a matrix algorithm.

Additionally, based on images acquired in dynamic renal scintigraphy between 40 and 140 s of a study, parametric clearance images (PAR) were also generated using an in-house developed software [4] applying a Rutland-Patlak analysis method [3].

For this purpose, renal curves were determined for every pixel making use of the following equation:

$$R_{ij}(t) = F_{ij}P(t) + K_{ij}\int_0^t P(\tau)d\tau \quad [1]$$

where $R_{ij}(t)$ denotes time — activity curve obtained from every pixel of a kidney region of interest; i, j are numbers of row and column in an image matrix; $P(t)$ defines changes of activity in blood (taken from ROI over a heart);

$$\int_0^t P(\tau)d\tau$$

is a cumulative activity that has flown through a heart from the moment of injection to time point t, K_{ij} stands for a coefficient proportional to a regional functional efficiency of a kidney (regional clearance value), $F_{i,j} P(t)$ denotes counts from vascular activity and $t < t_{max}$, where t_{max} is a time point when a radiopharmaceutical begins its outflow from a kidney.

Dividing both sides of Eq. (1) by $P(t)$, gives following equation:

$$\frac{R_{ij}(t)}{P(t)} = F_{ij}P(t) + K_{ij}\frac{\int_0^t P(\tau)d\tau}{P(t)} \quad [2]$$

where $K_{i,j}$ plays a role of a slope coefficient. Its values, proportional to regional renal clearance, were calculated from a linear part of a Rutland-Patlak plot (for all rows and columns) and formed a parametric clearance image.

This algorithm calculated, for every image pixel, a parameter proportional to a local value of renal clearance, was presented in shades of grey. In this way image presenting regional values of clearance function in every image pixel was obtained. A local impairment of this function could be observed in form of a shift of grey shade, proportional to its severity.

Radiopharmaceutical uptake in SUM images and a regional distribution of clearance function in PAR images were analyzed, after one smoothing, on a monitor in a grey scale by two experienced nuclear medicine specialists in three segments of each kidney: upper, medium and lower, and a final result was attained in the form of consensus. Image interpreters were blinded to the location of ESWL intervention.

Results of this analysis were grouped into two categories:
1. Normal (N) — without lesions of uptake/clearance function impairment;
2. Abnormal (AB) — with lesion(s) of uptake/clearance function impairment which was further subdivided into two categories with regard to abnormality extent:
   a. Kidneys with local (L) damage confined to one segment,
   b. Kidneys with diffused (D) damage in two adjacent segments or a whole organ.

Statistical analysis

Quantitative data were described by mean values and standard deviations, qualitative data — by frequencies of occurrence.

Distributions of frequencies were compared by Pearson χ^2 test, for paired data (visual assessment before and after ESWL) McNemar's test was applied.

Hypothesis about distributions of quantitative parameters of kidney function were tested by non-parametric methods — Mann-Whitney U test for independent groups and Wilcoxon test — for paired data (before and after ESWL).

Statistical significance was considered achieved for a value of $p \leq 0.05$.

All the calculations were derived with Statistica 10.0 software.

Results

In dynamic renal scintigraphy performed before ESWL in none of 40 kidneys subject to later intervention functional defects in PAR and SUM images were detected (Figure 1).

Local clearance function defects detected in PAR and SUM images were always observed in segments corresponding to location of calculus and ESWL target, although in several cases were more extensive. No local function defects located at sites incompatible with ESWL targets were detected. In a study performed a week after ESWL abnormal clearance function in PAR images was detected in 19 out of 40 (48%) kidneys after intervention. In 12 kidneys a local damage was detected in a segment (upper, medium or lower) where a calix with calculus subject to acoustic wave shock was located (in case of calculus in renal pelvis functional abnormalities were located in medium or lower segments) (Figure 2). In 7 kidneys impairment of clearance function in PAR images was diffused (D): in 4 kidneys, beside a segment of calculus location, it was also observed in adjacent segment (if a calculus was located in renal pelvis, medium and lower segments were affected) and in case of 3 kidneys whole organs (all 3 segments) were affected, probably in a mechanism or a renal stunning (Figure 3). Altogether lesions of functional impairment were detected in 29 out of 57 (51%) segments of these kidneys. In a study performed a month after ESWL abnormalities were detected in 16 out of 40 (40%) kidneys and they were less extensive. Local functional impairment confined to one segment was revealed in 15 kidneys and diffused — in 1 kidney (in 2 segments). Clearance function impairment in PAR images affected 17 out of 48 (35%) segments.

Radiopharmaceutical uptake function abnormalities detected in SUM images a week as well as a month after ESWL were detected in significantly lower numbers of kidneys as compared with PAR im-
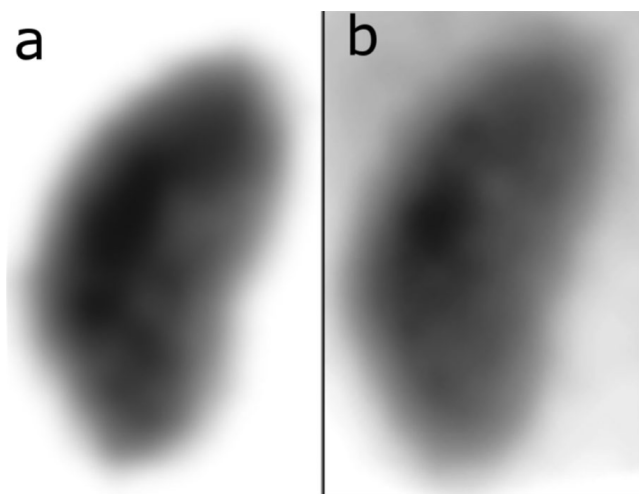

Figure 1. Normal images of a left kidney before ESWL: **A**. parametric (PAR) and **B.** summation (SUM)
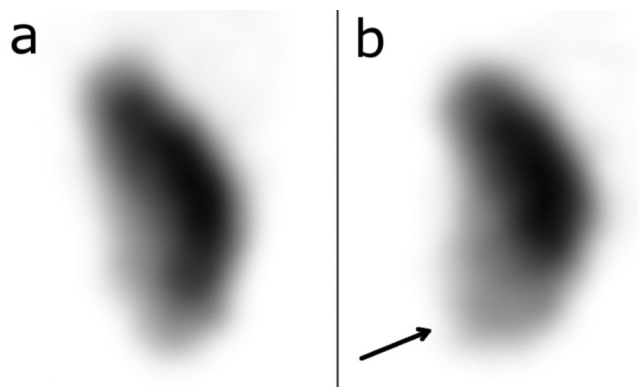

Figure 2. Parametric images (PAR) of a right kidney: **A.** before ESWL; **B.** one week after intervention. Local defect visible in a lower segment (arrow) after ESWL of a calculus located in the inferior calyx
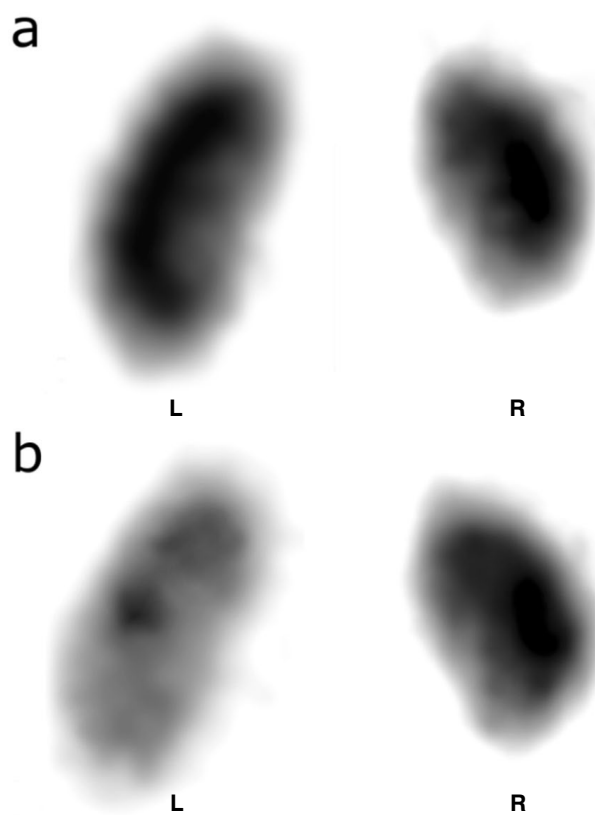

Figure 3. Parametric images (PAR) of kidneys: **A.** before ESWL of a left kidney and **B.** one week after intervention. Diffused function impairment of a whole kidney after ESWL of a calculus located in a calyx; L — left kidney; R — right kidney

ages — 6 vs. 19 (p = 0.002) and 5 vs. 16 (p = 0.003), respectively (Table 1 and Figure 4).

A global function of kidneys with abnormal PAR images obtained a week after EWSL, in which clearance function defects were observed in 51% (29/57) of segments, was significantly worse than a function of kidneys with normal PAR images. Mean RSF was significantly lower and MTT and PTT were significantly higher for abnormal kidneys than normal in PAR images (Tab. 2). However, in a study performed a month after ESWL, when clearance function defects were still observed, although only in 35% (17/48) of segments, global function parameters of kidneys with abnormal PAR were improved, their mean values already did not differ between kidneys with abnormal and normal PAR images.

Discussion

A typical dynamic radionuclide study shows a distribution and movement of a radiopharmaceutical through examined organ, thus revealing its function in a direct way. Additional processing of such a study allows to generate parametric images providing regional distribution of examined parameter, reflecting organ function in an indirect but more in-depth way.

Parametric images were introduced first by Adam and Geffers [14, 15] generating maps of several hemodynamic parameters of a heart. Parametric images are still considered a standard addition to a radionuclide ventriculography.

Articles on application of parametric images in detection of renal function impairment can be met only occasionally. Gordon et al. were the first ones to apply such dynamic renal study processing and prove its usefulness in detection of renal scarring [16]. Similar results were obtained in our department with additional high reproducibility of image grading [4]. Moreover, our study revealed that local impairment of renal function observed in parametric images may be an early symptom of nephropathy in type 1 diabetes [17].

Works applying radionuclide methods in the assessment of functional consequences of lithotripsy are rare. Lechevaillier et al. [18] applied a static renal study (^{99m}Tc-DMSA SPECT) for the evaluation of 12 kidneys before and 30 days after ESWL. They revealed minor tracer uptake defects around foci of post ultrasound shock wave sites. The same authors and also Lottman et al. [19] detected cases of renal scars after ESWL in adults as well as children. Using a dynamic renal scintigraphy and radionuclide methods for calculation of glomerular filtration rate (GFR) and effective renal plasma flow (ERPF) an impairment of global renal function directly after ESWL was observed that usually resolved subsequently.

A transient prolongation of mean and parenchymal transit times (MTT and PTT) after ESWL was shown amongst others by Eterovic et al. [10], Ilgin et al. [20] and Bomanji et al. [21]. A reduction of split function was also demonstrated by Kande et al. [22] and Gupta et al. [23]. Transient reductions of GFR and ERPF values in kidneys after ESWL were also revealed [10, 11, 24].

Table 1. Comparison of renal function disturbances (L — local or D — diffused) in parametric (PAR) and conventional (SUM) images

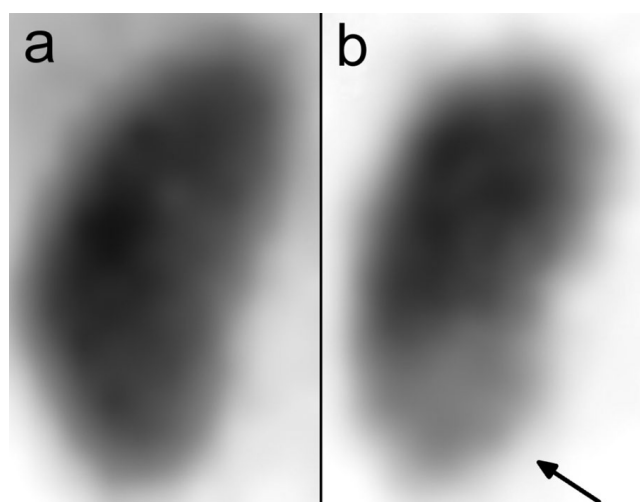|	Abnormal parametric images		p
	PAR	SUM	
Week after ESWL	19 (48%)	6 (15%)	0.002
	[12L, 7D]	[3L, 3D]	
Month aftre ESWL	16 (40%)	5 (13%)	0.003
	[15L, 1D]	[4L, 1D]	

Figure 4. A. Summation (SUM) and **B.** parametric images of a left kidney one week after ESWL of a calculus located in the inferior calyx. Local defect in a lower segment visible only in PAR image (arrow)

Table 2. Renal function parameters (SF, MTT, PTT) one week and one month after ESWL in patients with abnormal and normal parametric images. Data are presented as mean ± st. dev.

	Week after ESWL			Month after ESWL		
	Abnormal	Normal	p	Abnormal	Normal	p
	n = 19	n = 21		n = 16	n = 24	
	s = 51%			s = 35%		
	(29/57)			(17/48)		
SF	42 ± 10	49 ± 8	0.036	44 ± 10	48 ± 6	0.40
MTT	297 ± 140	190 ± 69	0.022	202 ± 72	206 ± 76	0.88
PTT	239 ± 125	132 ± 18	0.0001	159 ± 67	142 ± 32	0.84

Only Konecki et al. [25] attempted to apply parametric clearance images in detection of regional function impairment in patients after ESWL. They analyzed 67 kidneys before therapy and in two control studies — a week and a month after the intervention. The first control study showed lesions of impaired clearance function in 40% of kidneys. In the second control study these areas were preserved in about ¼ of kidneys but were less severe.

In the present study, due to patient selection, PAR and SUM images of all 40 kidneys before ESWL were normal. We showed that one week as well as one month after therapeutic intervention PAR images revealed local impairments of renal function around foci of ultrasound shock wave in significantly more kidneys than SUM images (Table 1). An advantage of PAR over SUM images in detection of local renal dysfunction should be attributed to the fact that PAR images present on a pixel by pixel basis distribution of relative values of a quantitative clearance parameter, in other words the clearance of blood from a nephrotropic radiopharmaceutical, in small fragments of renal parenchyma.

Local defects of renal function in PAR images, detected one week after ESWL in 19 kidneys, were observed in about a half of all segments of those kidneys and were as extensive as to be reflected in the impairment of their global function. Mean values of SF, MTT and PTT were significantly worse than for the remaining kidneys with normal PAR images.

In studies performed a month after ESWL lesions of function impairment found in 16 kidneys in PAR images were less extensive (in 15 cases changes were only local and altogether included about $\frac{1}{3}$ of renal segments). Mean values of global functional parameters obtained for those kidneys (SF, MTT and PTT) did not differ significantly from values obtained for kidneys with normal PAR images. It appears that a local renal dysfunction detected in PAR images a month after ESWL was not severe enough to be reflected in values of conventional parameters describing global renal function.

Conclusions

Parametric renal clearance images enhance diagnostic potential of a dynamic renal scintigraphy with detection of local function defects. In studies performed a week and a month after ESWL parametric clearance images revealed more cases of local renal function impairment than images obtained by conventional summation. The reliability of parametric images obtained a week after ESWL was confirmed by significantly worse values of global renal function parameters. Parametric images obtained a month after ESWL still allowed to reveal in some kidneys less severe lesions of regional function impairment that were not reflected in parameters of renal global function.

References

1. Oppenheim BE, Appledorn CR. Parameters for functional renal imaging. In: Esser PD. ed. Functional Mapping of Organ Systems and Other Computer Topic. Society of Nuclear Medicine, New York 1981: 39–55.
2. Szabo Z, Kutkuhn B, Georgescu G, et al. Parametrische Darstellung der Nierenfunktion mit 99mTc-Merkaptoazetyltriglyzin (MAG3). Nucl Med. 1989; 28: 73–83.
3. Rutland MD. A comprehensive analysis of renal DTPA studies. I. Theory and normal values. Nucl Med Commun. 1985; 6(1): 11–20, doi: 10.1097/00006231-198501000-00003, indexed in Pubmed: 3916534.
4. Kuśmierek J, Pietrzak-Stelmasiak E, Bieńkiewicz M, et al. Diagnostic efficacy of parametric clearance images in detection of renal scars in children with recurrent urinary tract infections. Ann Nucl Med. 2015; 29(3): 313–318, doi: 10.1007/s12149-014-0944-4, indexed in Pubmed: 25563578.
5. Brewe SI, Atala AA, Ackerman DM, Steinboc GS. Shock wave lithotripsy damage in human cadaver kidneys. J Endourol. 1988; 2(4): 333–339, doi: 10.1089/end.1988.2.333.
6. Seitz G, Pletzer K, Neisius D, et al. Pathologic-Anatomic Alterations in Human Kidneys after Extracorporeal Piezoelectric Shock Wave Lithotripsy. J Endourol. 1991; 5(1): 17–20, doi: 10.1089/end.1991.5.17.
7. Umekawa T, Kohri K, Yamate T, et al. Renal damages after extracorporeal shock wave lithotripsy evaluated by Gd-DTPA-enhanced dynamic magnetic resonance imaging. Urol Int. 1992; 48(4): 415–419, doi: 10.1159/000282366, indexed in Pubmed: 1413304.
8. Rubin JI, Arger PH, Pollack HM, et al. Kidney changes after extracorporeal shock wave lithotripsy: CT evaluation. Radiology. 1987; 162(1 Pt 1): 21–24, doi: 10.1148/radiology.162.1.3786764, indexed in Pubmed: 3786764.
9. Clark DL, Connors BA, Evan AP, et al. Localization of renal oxidative stress and inflammatory response after lithotripsy. BJU Int. 2009; 103(11): 1562–1568, doi: 10.1111/j.1464-410X.2008.08260.x, indexed in Pubmed: 19154498.
10. Eterović D, Juretić-Kuscić L, Capkun V, et al. Pyelolithotomy improves while extracorporeal lithotripsy impairs kidney function. J Urol. 1999; 161(1): 39–44, doi: 10.1097/00005392-199901000-00014, indexed in Pubmed: 10037363.
11. Thomas R, Roberts J, Sloane B, et al. Effect of Extracorporeal Shock Wave Lithotripsy on Renal Function. J Endourol. 1988; 2(2): 141–144, doi: 10.1089/end.1988.2.141.
12. Piepsz A, Kinthaert J, Tondeur M, et al. The robustness of the Patlak-Rutland slope for the determination of split renal function. Nucl Med Commun. 1996; 17(9): 817–821, doi: 10.1097/00006231-199609000-00014, indexed in Pubmed: 8895911.
13. Cichocki P, Surma M, Woźnicki W, et al. Preliminary assessment of interand intraobserver reproducibility, and normative values of renal mean transit time (MTT) and parenchymal transit time (PTT) for 99mTc-etylenodicysteine. Nucl Med Rev Cent East Eur. 2015; 18(1): 29–34, doi: 10.5603/NMR.2015.0007, indexed in Pubmed: 25633514.
14. Geffers H, Adam WE, Bitter F, et al. Radionuklid — Ventrikulographie. I. Grundlagen und Methoden. Nucl Med. 1978; 17: 206–210.
15. Adam WE, Tarkowska A, Bitter F, et al. Equilibrium (gated) radionuclide ventriculography. Cardiovasc Radiol. 1979; 2(3): 161–173, doi: 10.1007/bf02552061, indexed in Pubmed: 498193.
16. Gordon I, Anderson PJ, Lythgoe MF, et al. Can technetium-99m-mercaptoacetyltriglycine replace technetium-99m-dimercaptosuccinic acid in the exclusion of a focal renal defect? J Nucl Med. 1992; 33(12): 2090–2093, doi: 10.1007/bf02426698, indexed in Pubmed: 1334134.
17. Frieske I, Surma MJ, Rogozińska-Zawiślak A, et al. Parametric clearance kidney scintigrams; diagnostic potential in diabetes. Nucl Med Rev Cent East Eur. 2007; 10(1): 16–20, indexed in Pubmed: 17694496.
18. Lechevallier E, Siles S, Ortega JC, et al. Comparison by SPECT of renal scars after extracorporeal shock wave lithotripsy and percutaneous nephrolithotomy. J Endourol. 1993; 7(6): 465–467, doi: 10.1089/end.1993.7.465, indexed in Pubmed: 8124338.
19. Lottmann H, Archambaud F, Helal B, et al. [Extracorporeal shockwave lithotripsy in children. Study of the effectiveness and renal consequences in a series of eighteen children]. Ann Urol (Paris). 1995; 29(3): 136–142, indexed in Pubmed: 7486849.
20. Ilgin N, Iftehar SA, Vural G, et al. Evaluation of renal function following treatment with extracorporeal shock wave lithotripsy (ESWL): the use of

whole-kidney, parenchymal and pelvic transit times. Nucl Med Commun. 1998; 19(2): 155–159, doi: 10.1097/00006231-199802000-00010, indexed in Pubmed: 9548200.

21. Bomanji J, Boddy SA, Britton KE, et al. Radionuclide evaluation pre- and postextracorporeal shock wave lithotripsy for renal calculi. J Nucl Med. 1987; 28(8): 1284–1289, doi: 10.1056/nejmc1209257, indexed in Pubmed: 3302133.

22. Kaude JV, Williams CM, Millner MR, et al. Renal morphology and function immediately after extracorporeal shock-wave lithotripsy. AJR Am J Roentgenol. 1985; 145(2): 305–313, doi: 10.2214/ajr.145.2.305, indexed in Pubmed: 3875231.

23. Gupta M, Bolton DM, Irby P, et al. The effect of newer generation lithotripsy upon renal function assessed by nuclear scintigraphy. J Urol. 1995; 154(3): 947–950, doi: 10.1016/s0022-5347(01)66940-4, indexed in Pubmed: 7637099.

24. Pourmand G, Baradaran N, Salem S, Ahmadi H, Mehrsai A, Hematian MA. Extracorporeal shock wave lithotripsy and its effect on renal function, assessed by 99m technetium diethylene-triamine-pentaacetic acid scintigraphy. J Urol. 2008; 179(4): 464, doi: 10.1016/s0022-5347(08)61363-4.

25. Konecki T, Frieske I, Kuśmierek J, et al. Parametric kidney clearance images — evaluation of regional renal function in patients undergoing corporeal shock wave lithotripsy (ESWL). Eur Urol. 2010;(9 suppl): 659–660 (abstr.).